The Journal of Headache and Pain

RESEARCH

Open Access

3T MRI thalamic segmentation reveals no macrostructural changes in interictal episodic migraine without aura compared to healthy controls

Irene Giardina[1*†], Antonio Di Renzo[2†], Davide Chiffi[3], Giada Giuliani[3], Gabriele Sebastianelli[4], Francesco Casillo[4], Chiara Abagnale[4], Lucia Ziccardi[2,5], Andrea Pucci[6], Vincenzo Parisi[2,7], Marta Altieri[3], Vittorio Di Piero[3], Gianluca Coppola[4] and Francesca Caramia[3]

Abstract

Background The thalamus plays a central role in the pathophysiology of migraine, particularly through its involvement in the thalamocortical network. Structural changes in this region may underlie the altered sensory processing observed in migraine. This study aimed to assess volumetric differences in the thalamus and its subregions between patients with episodic migraine without aura and healthy controls, using MRI acquired during the interictal phase.

Methods Thirty patients with episodic migraine without aura (MO) and 30 healthy controls (HCs) of comparable age and sex underwent high-resolution T1-weighted MRI and full ophthalmological evaluation. All patients were scanned during the interictal phase and were not receiving preventive treatment. Volumetric segmentation made using FreeSurfer's automatic segmentation software (v7.4.1) included the entire thalamus and 25 subregions. General linear models were used to assess volumetric differences, controlling for age, sex, and total intracranial volume.

Results No statistically significant differences were found in the total thalamic volume or in any of its subregions between MO patients and HCs ($p_{uncorrected}$ >0.05). Moreover, no correlations emerged between thalamic volumes and clinical characteristics of migraine (attack frequency, attack duration, severity of pain, HIT-6, MIDAS, ASC-12, and days since the last attack, $p_{FDR\ corrected}$ >0.05). No relevant ophthalmological abnormalities were detected.

Conclusions Our findings suggest that thalamic macroscopic volumes are not altered during the interictal phase in patients with MO and without relevant ocular abnormalities. Complementary approaches—such as functional or microstructural imaging—may be required to further elucidate thalamic involvement in migraine pathophysiology.

Keywords FreeSurfer, Thalamus, Segmentation, Migraine, MRI

†Irene Giardina and Antonio Di Renzo contributed equally to this work.

*Correspondence:
Irene Giardina
i.giardina@uniroma1.it

Full list of author information is available at the end of the article

Introduction

A substantial amount of evidence indicates that the thalamus is critically involved in the pathophysiology of migraine, as emphasized by recent advances in neuroimaging and electrophysiology [1, 2].

The failure of thalamocortical drive appears to underlie the electrical anomalies observed in the migraine-affected brain [3]. During the interictal period of migraine, visual and somatosensory high-frequency thalamocortical activity has been shown to be altered [1, 4, 5] and correlated with the degree of lateral inhibition in the somatosensory cortex [6]. The amplitude of thalamocortical loop activity exhibited a substantial correlation with the clinical progression of migraine, as spontaneous exacerbation was linked to diminished drive activity, whereas spontaneous amelioration was connected with increased drive activity [7].

Findings from animal models suggest that the thalamus mediates the antinociceptive response to common acute [8, 9] and preventive [10–12] migraine treatments and may significantly influence the development of sensory hypersensitivity to visual stimuli, particularly concerning the pulvinar subnucleus [13]. The BOLD signal in the pulvinar, measured using functional MRI during a session of 15 pain stimuli, was found to be bilaterally increased in interictal migraine patients compared to the decreased signal in healthy controls [14]. In another fMRI study, the BOLD signal of the mediodorsal thalamic subnucleus was increased in individuals with vestibular migraine and positively correlated with attack frequency [15].

From a structural and morphological perspective, numerous human studies have reported specific thalamic alterations in migraine, using different MRI-based analysis approaches. Abnormal microstructural diffusive metrics were detected in the thalamic nuclei during interictal migraine, correlating with the time elapsed since the most recent attack [16–18]. Magon et al. [19] examined migraine patients in the interictal phase using multi-atlas automated segmentation and deformation-based morphometry, revealing significant volume reductions in specific nuclei related to the limbic system—including dorsal anterior, central, and lateral regions— compared to healthy controls. They found no shape changes or associations with attack frequency or duration [19]. However, some of their patients were on preventive medications for migraine that, according to previous studies, may alter structure and function of their brain and the clinical progression of the disease [20–26]. Another volumetric study reported generalized brain volume reduction, including the thalamus, in patients with both episodic and chronic migraine, although it did not specify the timing of MRI in relation to the migraine cycle and the inclusion of patients under migraine prevention [27]. Shin et al. utilized FreeSurfer to segment thalamic subnuclei in a cohort of MO patients, revealing increased volumes of the right anteroventral nucleus and bilateral medial geniculate nuclei, alongside decreased volumes of the bilateral parafascicular nuclei compared to healthy controls [28]. In Shin et al. (2019), patients were scanned during headache-free intervals; however, the occurrence of migraine attacks in the days preceding or following the scanning session was not explicitly assessed. This leaves open the possibility that some patients may have been scanned during the peri-ictal phase, a period characterized by potential fluctuations in cerebral metabolic and functional activity [29–32].

The aim of our study was to investigate the volume of the thalamus and its subregions performing 3T MRI and using FreeSurfer's automatic segmentation software [33] in a well-characterized sample of patients with episodic migraine without aura (MO), scanned during the interictal phase and not receiving preventive medication, compared to a group of healthy controls (HCs). This study intentionally focused on preventive-naïve patients with episodic migraine without aura scanned interictally to minimize clinical and pharmacological heterogeneity and to isolate disease-related macrostructural effects. We further regressed the volume of the thalamus and its subregions with patients' clinical features, such as attacks frequency, attacks duration, severity of pain, HIT-6, MIDAS, ASC-12, and days since the last attack. Furthermore, as prior MRI studies indicated structural anomalies associated with neuro-ophthalmological disorders [34], we conducted a series of tests to exclude patients with these conditions.

We tested the hypothesis that the thalamic volume and its subregions may differ between MO patients and HCs, and that these volumetric measures may correlate with clinical migraine characteristics.

Methods

Participants

A total of 60 participants were prospectively enrolled. Thirty patients (Table 1) diagnosed with episodic MO were recruited from the Headache Centres of Rome and Latina. Diagnosis was established according to the International Classification of Headache Disorders (ICHD III) [35]. Patients underwent MRI scans during the interictal phase, defined as at least three consecutive days without migraine attacks before and after the scan, as confirmed through follow-up phone interviews made ≥ 4 days after the day of the scan. Patients experienced unilateral or bilateral migraine headaches but did not consistently report pain on the same side for every attack. Patients receiving preventive treatment within the previous three months were excluded. Other primary or secondary headache types were ruled out through clinical and/or instrumental evaluation, if necessary. We excluded

Table 1 Demographic and clinical characteristics of healthy controls (HCs) and patients with migraine without aura scanned during migraine-free intervals (MO)

	HCs ($n=30$)	MO ($n=30$)	Statistics
Women (n)	23	25	$Chi^2=0.417$, $p=0.519$
Age (years)	28.40 ± 8.36	32.17 ± 10.89	t = -1.50, $p=0.138$
Disease duration (years)		6.9 ± 8.3	
Attack frequency/month (n)		5.7 ± 3.0	
Attack duration (hours)		33.7 ± 20.0	
Days from the last migraine attack (n)		7.3 ± 2.8	
Number of days with acute medication intake/month (n)		4.5 ± 2.5	
MIDAS		20.7 ± 16.8 Q1-Q3: 15.25-21.00	
HIT-6		61.2 ± 7.6 Q1-Q3: 58.75-64.00	
ASC-12		4.3 ± 4.1 Q1-Q3: 2.75–5.25	

Data are presented as mean ± standard deviation, with interquartile ranges (Q1–Q3) additionally reported for MIDAS, HIT-6, and ASC-12 due to non-normal distribution. Group differences were tested using student's t-test or Chi-square test as appropriate

patients with a history of other neurological diseases, metabolic disorders, systemic hypertension, and connective, autoimmune or neuro-ophthalmological diseases (such as glaucoma or optic neuritis). Indeed, all subjects underwent full ophthalmological evaluation including best-corrected visual acuity measurements (Snellen Equivalent), slit-lamp biomicroscopy for anterior segment examination, indirect ophthalmoscopy after pupil dilation (tropicamide 1% drops) for posterior segment examination, and Goldmann applanation tonometry for intraocular pressure (IOP) measurement and chromatic perception testing by Ishihara plates.

The use of symptomatic medication was not allowed on the day of the scan. Out of the 40 patients initially recruited, 10 were excluded according to our exclusion criteria: 4 experienced a migraine attack during the examination, 1 was excluded due to the identification of a minor aneurysm, and 5 were omitted due to a finding of white matter hyperintensity.

Thirty HCs of comparable age and sex were recruited from among medical students and healthcare professionals for comparative analysis. This strategy was adopted to allow strict health screening and reduce potential systemic or neurological comorbidities that could confound morphometric analyses. They displayed no evident medical or relevant ophthalmological conditions, personal or familial history of primary headaches or epilepsy, nor regular substance use. All recruited subjects were right-handed.

Female participants were consistently scanned at mid-cycle. All scanning sessions were conducted in the afternoon (4:00–7:00 p.m.). Participants were instructed to avoid sleep deprivation and alcohol use on the day prior to scanning. Caffeinated drinks were prohibited on the day of the scan. Additional exclusion criteria for both HCs and MO were the presence of structural brain abnormalities on MRI. All participants received a detailed explanation of the study and provided written informed permission. The study protocol was approved by the Ethical Committee of the Faculty of Medicine, Sapienza University of Rome (Protocol No. 0295/2023).

MRI protocol

All participants underwent MRI on a 3 Tesla Siemens Magnetom Vida scanner, using a 32-channel head coil. High-resolution T1-weighted sagittal magnetization-prepared rapid gradient echo (MPRAGE) sequences were acquired (TR: 2300 ms, TE: 2.25 ms, 208 sagittal slices, voxel dimensions $0.8 \times 0.8 \times 0.8$ mm^3, base resolution 320, field of view 256 mm, slice thickness 0.8 mm).

Imaging data processing: thalamus subunits analysis

Thalamic segmentation was conducted using a functionality available in FreeSurfer 7.4.1 (https://surfer.nmr.mgh.harvard.edu/fswiki/SubregionSegmentation), a Python program that segments the thalamus into 25 nuclei, using a probabilistic atlas based on histological data [33].

Two expert researchers (F.C. and I.G.) carefully inspected each participant's and thalamus segmentations, eventually discarding those with artifacts; none of the thalamus segmentation was inaccurate.

The thalamic structure was partitioned into right and left subunits: anteroventral, laterodorsal, lateral posterior, ventral anterior, ventral anterior magnocellular, ventral lateral anterior, ventral lateral posterior, ventral posterolateral, ventromedial, centromedian, central lateral, paracentral, reuniens (medial ventral), mediodorsal medial magnocellular, mediodorsal lateral parvocellular, lateral geniculate, limitans (suprageniculate), paratenial, pulvinar anterior, pulvinar medial, pulvinar lateral, pulvinar inferior, medial geniculate nucleus, parafascicular, central medial; their volumes were calculated and recorded for each participant in the group (see Fig. 1).

Descriptive and inferential statistics were evaluated, focusing our attention on volumetric differences between groups and relationships assessments between volumes and clinical variables in MO group using SPSS for Windows (v.21 IBM corp.).

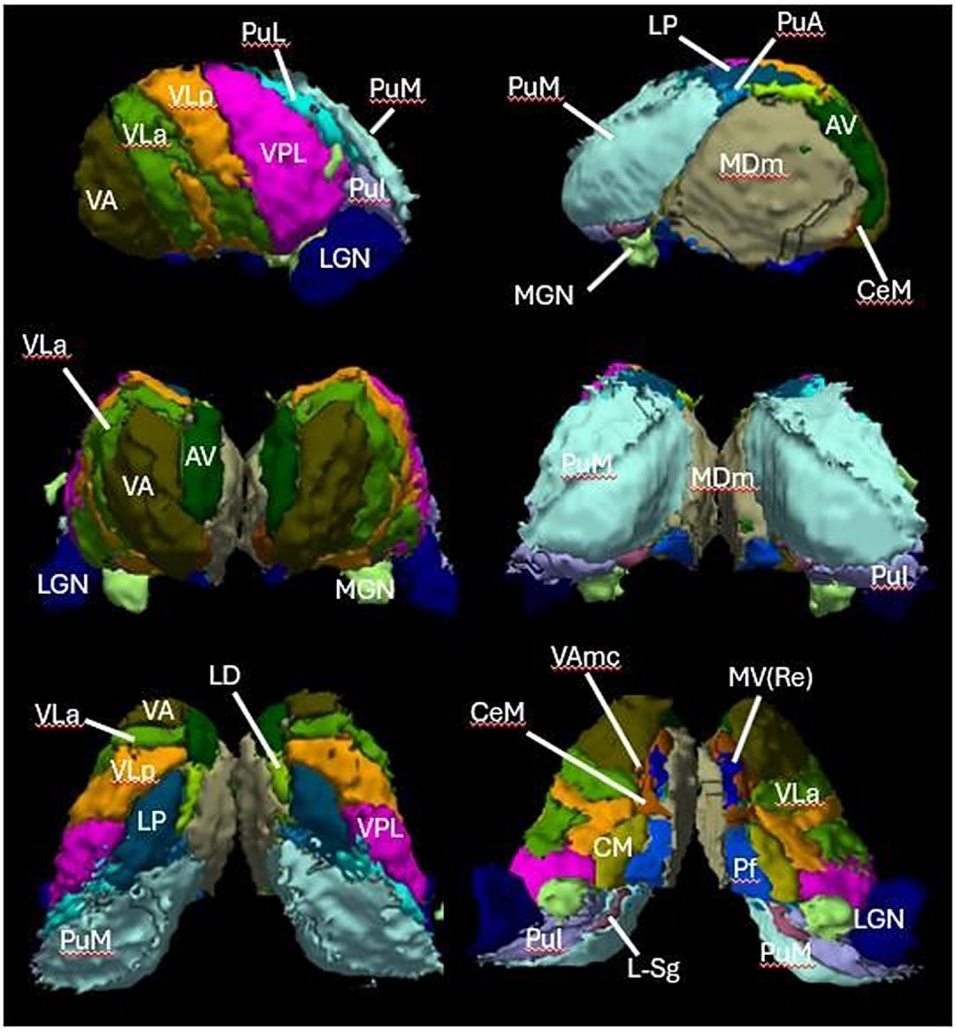

Fig. 1 Thalamic nuclei segmentation. FreeSurfer 3D rendering of thalamic nuclei in their lateral-medial (top row), ventral-dorsal (middle row) and caudal-rostral (bottom row) aspects on T1-weighted multiecho MPRAGE data of a representative sample subject. Lateral geniculate nucleus (LGN), Medial geniculate nucleus (MGN), Pulvinar inferior (Pul), Pulvinar medial (PuM), Limitans (Suprageniculate) (L-Sg), Ventral posterolateral (VPL), Centromedian (CM), Ventral lateral anterior (VLa), Pulvinar anterior (PuA), Mediodorsal medial (MDm), Parafascicular (Pf), Ventral anterior magnocellular (VAmc), Mediodorsal lateral (MDl), Central medial (CeM), Ventral anterior (VA), Reuniens (medial ventral) (MVre), Ventromedial (VM), Central lateral (CL), Pulvinar lateral (PuL), Paratenial (Pt), Anteroventral (AV), Paracentral (Pc), Ventral lateral posterior (VLp), Lateral posterior (LP), Laterodorsal (LD)

The TIV of each participant also was computed using FreeSurfer (version 7.4.1) [36–44]. A general linear model (GLM) was constructed, utilizing the subnuclei volumes of each participant's group as the dependent variables, while age and total intracranial volume (TIV) served as covariates (independent variables), with sex and group as factors, to assess any variations between groups.

A new GLM was developed to evaluate the correlation between the MO group volume of each thalamic subunit (dependent variables) and each clinical variable (covariates of interest), while adjusting for age and TIV (covariates of no interest) and including sex as a factor.

The Anderson-Darling and/or Kolmogorov-Smirnov tests were conducted for each model's covariate and responses to evaluate normality distributions.

P-values were set up at 0.025 (Bonferroni correction) for the volume differences between groups of the entire thalamus (left and right) and its subunits at $p < 0.05$, adjusted for multiple comparisons by the Benjamini-Hochberg method.

Finally, p-values were adjusted to a 0.05 false discovery rate (Benjamini-Hochberg) to account for multiple comparisons arising from the number of regions of interest and clinical factors assessed ($N = 7$).

Clinical variables included attack frequency (n/month), attack duration (hours), pain severity (0–10 visual analogue scale), HIT-6, MIDAS, ASC-12, and days (n) since the last attack.

Results

Table 1 presents the demographic and clinical characteristics of HCs and patients with interictal MO. No statistically significant differences in age or sex distribution were observed between groups. None of the patients had a migraine attack within the three days following the MRI scan, as confirmed by a follow-up telephone call conducted ≥ 4 days after the day of the scan.

Table 2 summarizes the volumes of the whole thalamus and its subregions in both hemispheres. No significant volumetric differences were found between MO patients and HCs for total thalamic volume (p_uncorrected > 0.05, Fig. 2) or any of the 25 bilateral thalamic subunits (p_uncorrected > 0.05).

A general linear model was also used to assess associations between thalamic volume and clinical measures (Table 3). No statistically significant correlations were observed between total thalamic volume and clinical variables (p_uncorrected > 0.05). Some subregional volumes showed uncorrected associations (p_uncorrected < 0.05), but none of these survived correction for multiple comparisons (p_FDRcorrected > 0.05; Table 4).

Finally, Table 5 reports the ophthalmological screening results. All participants, both HCs and MO patients, showed clear optical media consistent in transparent cornea and absence of any lens opacity (i.e. absence of cataract) at the anterior segment examination. No subject reported a history of glaucoma (IOP values were within normal values). At the observation of the posterior segment, neuroophthalmological diseases (as optic neuritis or optic nerve edema) or macular/retinal disorders (like retinal detachment, central serous chorio-retinopathy, macular hole) were not found.

Discussion

Our results indicate the absence of statistically significant differences in the macrostructural features of thalamic grey matter between patients with migraine without aura (MO) and healthy controls (HCs). Furthermore, no associations were found between thalamic macrostructural measures and migraine clinical characteristics.

This study examined the thalamus and its 25 subnuclei using FreeSurfer automatic segmentation software, which relies on a probabilistic atlas derived from histological analysis of the thalamus, combining magnetic resonance imaging and histological data through a 3D reconstruction informed by blockface images and enhanced via in vivo MR segmentations. The resultant atlas, depicted as an adaptive tetrahedral mesh, had significant concordance with classical histological data and showed excellent reliability in automated segmentation tasks [33]. We meticulously verified that MO patients were scanned during the interictal phase and not in the peri-ictal phase, meaning they had not experienced attacks in the three days preceding and following the examination. To further reduce clinical heterogeneity, we focused exclusively on episodic MO; accordingly, our conclusions pertain to this phenotype and are not intended to generalize to migraine with aura. Moreover, we rigorously excluded patients receiving prophylactic treatment for migraine or presenting neuro-ophthalmological disorders. This is due to previous MRI studies revealing structural abnormalities linked to neuro-ophthalmological conditions [34] and the fact that including patients on preventive migraine medications may not only influence the clinical progression of the disease but also modify both the structure and function of the migraine-affected brain, potentially biasing the study's results either directly or indirectly. Current evidence indicates that preventive medications frequently employed for migraine management, including beta-blockers, antiepileptics, and monoclonal antibodies targeting the calcitonin gene-related peptide (CGRP), may modify the structure and function of the migraine-affected brain [20–24]. Moreover, disease progression might lead to distinct patterns of functional activity, whether it is beneficial or unfavourable [25, 26].

While a prior investigation revealed microstructural abnormalities at the thalamic level through DTI sequences (notably, increased fractional anisotropy and decreased mean diffusivity) [16, 18], the findings of the current study indicate that microstructural alterations may not be associated with macrostructural volumetric changes in grey matter.

A previous study similarly examined patients with MO during the interictal phase using FreeSurfer for segmentation. Increased volumes of the right anteroventral nucleus and bilateral medial geniculate nuclei, alongside decreased volumes of the bilateral parafascicular nuclei, were detected in 35 patients with migraine compared to 40 HCs [28]. Nonetheless, their statistical analysis did not consider essential factors such as age and sex, and model fit indices were not reported, unlike our study, which utilized a stringent statistical methodology including these covariates. By contrast, our study applied rigorous statistical modeling, including these covariates, and additionally verified the interictal status of patients with structured screening around the scanning session. Naguib et al. [27] used FreeSurfer with 1.5 Tesla MRI and analyzed T1-weighted images alongside T2 and FLAIR sequences to evaluate grey and white matter structures, including the thalami, in patients with 14 episodic and 11 chronic migraine patients. Although their study did not focus on thalamic subunits, did not report the migraine phase during scanning, and employed lower field strength, they reported thalamic volume reductions only when episodic and chronic patients were combined. These effects disappeared when the groups were analyzed separately.

Table 2 Mean volumes (mm^3) ± standard deviations and interquartile ranges (25th–75th percentile) of thalamic subunits and total right and left thalamus in patients with episodic migraine without aura (MO) and healthy controls (HCs)

	Left			Right		
	HCs	MO	Inferential statistics	HCs	MO	Inferential statistics
Lateral geniculate nucleus (LGN)	305.22 ± 47.45 269.31–337.41	272.98 ± 43.08 246.85–314.16	F = 2.48; *p* = 0.12	306.09 ± 40.41 277.06–328.35	277.99 ± 48.95 244.41–311.91	F = 1.96; *p* = 0.17
Medial geniculate nucleus (MGN)	118.15 ± 22.45 100.41–134.34	109.28 ± 15.76 101.03–115.60	F = 1.11; *p* = 0.30	127.89 ± 22.88 106.43–140.36	120.64 ± 17.22 109.90–132.67	F = 0.67; *p* = 0.42
Pulvinar inferior (PuI)	262.65 ± 44.29 227.99–293.65	243.33 ± 38.26 218.25–265.90	F = 0.01; *p* = 0.91	287.85 ± 46.71 259.83–312.55	264.23 ± 42.33 233.57–293.50	F = 0.35; *p* = 0.56
Pulvinar medial (PuM)	1197.10 ± 165.10 1065.60 – 1319.50	1130.20 ± 132.00 1031.4 -1239.30	F = 0.00; *p* = 0.95	1312.10 ± 176.00 1156.1–1455.50	1219.7 ± 142.30 1075.8-1343.60	F = 0.40; p = 0.53
Limitans (Suprageniculate) (L-Sg)	25.58 ± 7.82 19.85–30.43	23.36 ± 4.74 18.81–27.82	F = 0.01; *p* = 0.93	23.18 ± 6.16 18.98–27.66	22.85 ± 4.38 19.92–25.17	F = 0.76; *p* = 0.39
Ventral posterolateral (VPL)	981.50 ± 192.70 834.80–997.70	914.60 ± 122.70 834.80–997.70	F = 0.09; *p* = 0.77	1029.70 ± 201.80 873.5–1181.40	1007.50 ± 152.0 886.20–1102.30	F = 0.85; *p* = 0.360
Centromedian (CM)	271.10 ± 42.65 234.38–293.33	253.09 ± 29.10 238.41–271.7	F = 0.30; *p* = 0.59	277.52 ± 46.78 240.52–304.32	262.98 ± 40.03 231.33–286.79	F = 0.00; *p* = 0.98
Ventral lateral anterior (VLa)	715.50 ± 119.10 638.30–762.30	645.60 ± 74.80 604.90–702.80	F = 1.39; *p* = 0.24	716.30 ± 103.1 637.70–786.30	665.70 ± 87.70 596.50–734.10	F = 0.14; *p* = 0.71
Pulvinar anterior (PuA)	247.07 ± 35.09 226.45–260.36	232.22 ± 27.87 213.74–252.19	F = 0.00; *p* = 0.95	262.27 ± 33.99 232.93–282.55	248.66 ± 30.10 220.51–272.11	F = 0.01; *p* = 0.91
Mediodorsal medial (MDm)	851.10 ± 128.90 813.00–943.80	823.50 ± 93.00 770.70–880.00	F = 0.51; *p* = 0.48	886.50 ± 87.10 834.20–963.10	843.50 ± 91.50 790.50–919.30	F = 0.33; *p* = 0.57
Parafascicular (Pf)	63.99 ± 12.28 56.51–74.35	59.51 ± 9.21 53.96–65.77	F = 0.45; *p* = 0.50	66.74 ± 12.42 60.17–72.87	65.69 ± 11.78 60.86–73.42	F = 0.81; *p* = 0.37
Ventral anterior magnocellular (VAmc)	37.00 ± 6.47 32.56–39.78	33.93 ± 3.60 31.02–36.06	F = 0.25; *p* = 0.62	38.38 ± 5.96 34.43–42.37	35.25 ± 4.48 31.84–39.04	F = 0.27; *p* = 0.61
Mediodorsal lateral (MDl)	318.20 ± 64.60 276.10–343.10	290.98 ± 38.25 266.83–304.64	F = 0.52; *p* = 0.47	315.61 ± 33.76 294.49–335.97	303.95 ± 32.37 287.95–329.38	F = 0.00; *p* = 1.00
Central medial (CeM)	79.64 ± 14.48 66.64–87.24	74.45 ± 9.62 66.53–84.09	F = 0.04; *p* = 0.85	82.48 ± 14.27 69.91–92.14	77.87 ± 11.26 68.69–86.28	F = 0.05; *p* = 0.85
Ventral anterior (VA)	483.10 ± 91.00 425.50–522.60	436.08 ± 51.03 391.60–467.95	F = 0.43; *p* = 0.51	464.40 ± 69.10 408.10–512.20	430.10 ± 58.60 383.70–473.50	F = 0.00; *p* = 0.97
Reuniens (medial ventral) (MVre)	15.73 ± 3.51 13.52–17.79	14.94 ± 2.28 12.98–16.36	F = 0.20; *p* = 0.66	17.13 ± 3.17 14.78–19.61	16.03 ± 2.74 14.19–18.33	F = 0.04; *p* = 0.84
Ventromedial (VM)	26.71 ± 6.70 21.98–29.96	25.54 ± 4.03 22.75–28.00	F = 0.06; *p* = 0.81	27.85 ± 6.22 23.33–32.15	27.86 ± 5.06 23.74–31.38	F = 1.12; *p* = 0.30
Central lateral (CL)	39.25 ± 8.12 32.64–44.84	37.41 ± 5.97 33.32–41.83	F = 0.02; *p* = 0.88	42.51 ± 9.57 34.88–49.69	38.28 ± 8.26 31.61–42.01	F = 0.84; *p* = 0.36
Pulvinar lateral (PuL)	210.74 ± 49.45 168.52–250.34	192.24 ± 33.77 165.43–221.78	F = 0.00; *p* = 0.97	220.28 ± 49.75 178.81–252.00	206.95 ± 37.33 178.83–229.84	F = 0.23; *p* = 0.64
Paratenial (Pt)	7.72 ± 1.32 6.61–8.56	7.10 ± 0.87 6.46–7.87	F = 0.60; *p* = 0.44	8.49 ± 1.40 7.25–9.55	8.09 ± 1.11 7.11–8.98	F = 0.04; *p* = 0.85
Anteroventral (AV)	152.80 ± 30.54 135.30–157.46	144.09 ± 17.23 130.53–158.17	F = 0.16; *p* = 0.69	161.93 ± 27.03 140.31–188.22	153.84 ± 20.31 137.01–167.72	F = 0.10; *p* = 0.76
Paracentral (Pc)	4.40 ± 0.70 3.83–4.95	4.08 ± 0.54 3.81–4.43	F = 0.38; *p* = 0.54	5.09 ± 0.77 4.56–5.62	4.72 ± 0.59 4.13–5.26	F = 0.40; *p* = 0.53
Ventral lateral posterior (VLp)	930.70 ± 153.70 818.60–983.60	843.40 ± 97.4 801.2–912.50	F = 1.31; *p* = 0.26	938.70 ± 142.30 827.30–1021.5	879.80 ± 118.00 787.40–969. 50	F = 0.02; *p* = 0.88
Lateral posterior (LP)	144.60 ± 25.12 128.74–161.63	129.79 ± 13.86 120.24–139.89	F = 1.98; *p* = 0.17	139.75 ± 24.42 124.95–154.96	130.51 ± 18.74 116.65–142.41	F = 0.02; *p* = 0.90
Laterodorsal (LD)	33.43 ± 8.75 25.50–40.41	32.00 ± 6.69 26.92–35.05	F = 0.00; *p* = 0.97	35.37 ± 8.94 28.08–43.68	32.65 ± 9.62 26.83–37.67	F = 0.26; *p* = 0.61
Whole thalamus	7553 ± 1132 6771–8070	6974 ± 728 6541–7591	F = 0.50; *p* = 0.49	7794 ± 1039 6941–8479	7345 ± 846 6566–8072	F = 0.02; p = 0.89

Results from general linear models (GLMs) assessing between-group differences are reported

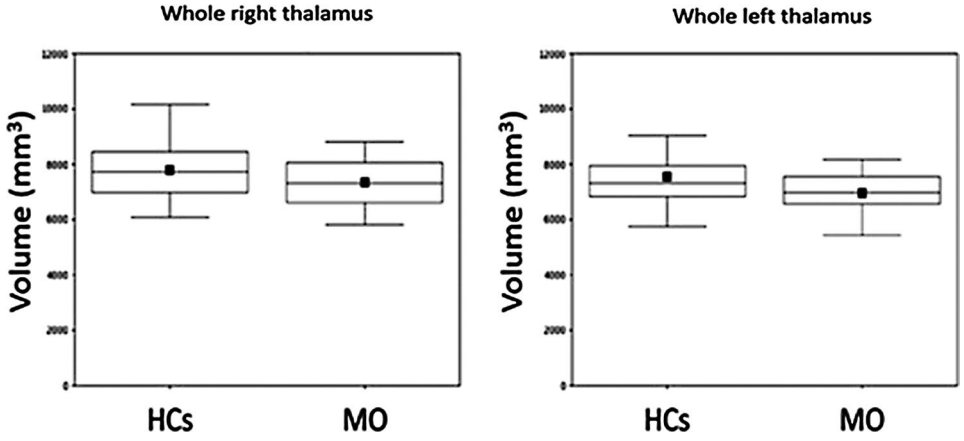

Fig. 2 Box-plots showing the volumes of the entire thalamus in both hemispheres in healthy controls (HCs) and patients with interictal migraine without aura (MO)

Other studies have used different methodological approaches. Magon et al. [19]. employed high-field 3 Tesla MRI and a multi-atlas segmentation algorithm (MAGeT Brain) in conjunction with deformation-based shape analysis. This method facilitated a detailed investigation of the volumes and shapes of thalamic subnuclei in 131 migraine patients versus 115 controls. Significant volumetric decreases were detected in nuclei involved in the cortico–subcortical network (including the central nuclear complex, anterior nucleus, and dorsolateral nucleus), as well as in striatal volume. No correlations between the volumes of thalamic nuclei and clinical variables were identified, aligning with our results. Details regarding preventive treatment status at scan and peri-scan attack monitoring were not specified, potentially introducing heterogeneity relative to our interictal, preventive-naïve sample [19].

In contrast, Matharu et al. [45] used voxel-based morphometry (VBM) with 2 Tesla MRI to investigate global and regional brain volume differences, including the thalamus, in 11 migraine with and 17 without aura patients. No macroscopic structural alterations were detected.

Overall, these methodological discrepancies underscore the difficulties in comparing volumetric and morphometric results across migraine neuroimaging research. FreeSurfer-based segmentation provides a reproducible and widely accessible method that complements multi-atlas and VBM approaches, enabling a detailed investigation of thalamic anatomy in episodic MO. Our work contributes to this effort by combining high-resolution imaging, advanced segmentation, and rigorous statistical modeling. Nonetheless, the absence of detected macrostructural anomalies in our patients does not rule out the involvement of the thalamus in migraine pathophysiology. Two resting-state functional MRI investigations identified modified thalamic connectivity with cortical regions during spontaneously occurring migraine episodes [46, 47]. A study investigated thalamic subregions in patients with interictal episodic migraine using a functional connectivity-based parcellation method (SPM12 and DPABI), revealing a reduction in functional connectivity between anterior, medial, and posterior thalamic subregions and brain areas predominantly associated with the medial pain processing system and the default mode network [48]. Other authors investigating the dynamic properties of thalamo-cortical networks in interictal migraine patients discovered a significant negative correlation between headache frequency and functional connectivity between the posterior thalamus and middle occipital gyrus, as well as a positive correlation with functional connectivity between the posterior thalamus and precuneus [49]. The interaction between the thalamus and cortex may predispose individuals to recurrent attacks, as evidenced by the correlation between abnormal low-frequency functional activity in the thalamus, particularly within its medial dorsal subnucleus, and the frequency of headache attacks in a mixed cohort of migraine patients with and without aura [50]. However, others observed augmented intrinsic functional connectivity of the thalami, with increased connection to frontal regions, which was inversely linked with headache severity [51].

In line with these observations, our results suggest that migraine recurrence may not induce plastic changes in thalamic volume, reinforcing the hypothesis that functional or microstructural—rather than macrostructural—alterations underlie thalamic involvement in migraine. Although no statistically significant group differences were detected, absence of evidence is not evidence of absence; the effect sizes (Table 6) indicate that any volumetric differences, if present, are likely small. By contrast, interictal DTI studies reported thalamic microstructural alterations (increased FA/decreased MD), sometimes varying with time since last attack [16, 18], suggesting

Table 3 Linear relationship between clinical variables and left and right thalamic volumes (F, p, R^2%)

	***N°* Attacks**	**Attacks duration**	**Severity of pain**	**HIT-6**	**MIDAS**	**ASC-12**	**Days since the last attack**
LGN (L/R)	(2.85; 0.14; 60.38) (3.07; 0.09; 44.78)	(0.13; 0.72; 56.10) (0.00; 0.96; 38.01)	(3.04; 0.09; 60.6) (5.50; 0.03; 49.20)	(0.09; 0.77; 56.02) (0.64; 0.43; 39.54)	(1.11; 0.30; 57.75) (2.50; 0.13; 43.64)	(0.07; 0.79; 55.99) (0.03; 0.87; 38.07)	(1.51; 0.23 58.39); (4.16; 0.05; 46.84)
MGN (L/R)	(2.55; 0.12; 40.22) (5.13; 0.03; 44.52)	(0.00; 0.98; 34.11) (1.51; 0.23; 36.94)	(4.63; 0.04; 44.40) (4.93; 0.03; 44.21)	(0.02; 0.89; 34.16) (0.93; 0.34; 35.52)	(0.03; 0.87; 34.19) (0.06; 0.81; 33.29)	(0.06; 0.81; 34.27) (1.22; 0.28; 36.25)	(0.21; 0.65; 34.66) (0.09; 0.77; 33.37)
PuI (L/R)	(0.02; 0.90; 63.50) (0.02; 0.88; 36.54)	(1.16; 0.29; 65.09) (0.84; 0.37; 38.56)	(0.87; 0.36; 64.71) (1.21; 0.28; 39.42)	(1.02; 0.32; 64.91) (0.12; 0.73; 36.78)	(4.48; 0.04; 69.03) (3.69; 0.04; 44.65)	(0.24; 0.63; 63.82) (1.29; 0.27; 39.60)	(0.13; 0.72; 63.67) (1.90; 0.18; 40.97)
PuM (L/R)	(0.38; 0.54; 56.61) (0.07; 0.79; 46.11)	(2.25; 0.15; 59.59) (0.01; 0.92; 45.97)	(1.19; 0.28; 57.96) (1.01; 0.32; 48.05)	(1.80; 0.19; 58.91) (0.01; 0.92; 45.98)	(1.69; 0.21; 58.74) (1.02; 0.32; 48.06)	(0.53; 0.47; 56.86) (0.17; 0.68; 46.32)	(0.48; 0.49; 56.78) (3.05, 0.09; 51.84)
L-Sg (L/R)	(1.86; 0.18; 33.44) (4.96; 0.04; 39.40)	(0.08; 0.78; 28.72) (0.01; 0.91; 28.07)	(0.19; 0.67; 29.03) (0.02; 0.89; 28.08)	(1.33; 0.26; 32.10) (0.04; 0.85; 28.13)	(0.78; 0.38; 30.67) (0.10; 0.76; 28.31)	(0.66; 0.42; 30.35) (0.04; 0.84; 28.14)	(1.28; 0.27; 31.97) (0.72; 0.40; 30.06)
VPL (L/R)	(0.70; 0.41; 35.59) (1.46; 0.24; 49.17)	(0.23; 0.63; 34.40) (0.37; 0.55; 46.99)	(0.16; 0.69; 34.22) (3.12; 0.09; 52.18)	(1.69; 0.21; 37.97) (0.75; 0.39; 47.78)	(0.56; 0.46; 35.23) (1.43; 0.24; 49.11)	(0.52; 0.48; 35.12) (0.70; 0.41; 47.68)	(0.62; 0.44; 35.37) (1.57; 0.22; 49.39)
CM (L/R)	(0.47; 0.50; 49.10) (3.04; 0.93; 45.49)	(1.72; 0.20; 51.47) (0.00; 0.95; 38.87)	(0.35; 0.56; 48.86) (4.65; 0.04; 48.45)	(3.51; 0.07; 54.53) (1.86; 0.18; 43.10)	(1.95; 0.17; 51.89) (0.99; 0.33; 41.19)	(0.00; 0.99; 48.14) (0.09; 0.76; 39.08)	(0.00; 0.95; 48.15) (0.00; 0.98; 38.86)
VLa (L/R)	(1.30; 0.27; 47.58) (2.79; 0.11; 62.29)	(0.07; 0.79; 45.03) (0.00; 0.971 58.09)	(0.01; 0.92; 44.89) (2.40; 0.14; 61.75)	(2.33; 0.14; 49.57) (1.24; 0.28; 60.06)	(0.16; 0.69; 45.22) (3.74; 0.07; 63.19)	(2.03; 0.17; 49.00) (0.13; 0.72; 58.31)	(2.05; 0.16; 49.05) (0.65; 0.43; 59.15)
PuA (L/R)	(0.14; 0.71; 49.33) (0.01; 0.91; 40.59)	(2.57; 0.12; 53.80) (0.72; 0.40; 42.23)	(3.06; 0.09; 54.60) (0.66; 0.42; 42.10)	(0.54; 0.47; 50.11) (0.01; 0.92; 40.59)	(0.15; 0.70; 49.35) (0.46; 0.50; 41.64)	(0.08; 0.78; 49.21) (0.05; 0.83; 40.67)	(1.23; 0.28; 51.43) (3.46; 0.28; 47.79)
MDm (L/R)	(0.42; 0.52; 19.91) (0.01; 0.91; 23.33)	(1.92; 0.18; 24.35) (0.19; 0.67; 23.86)	(0.79; 0.38; 21.06) (0.93; 0.34; 26.05)	(1.92; 0.18; 24.35) (0.00, 0.92; 23.29)	(2.79; 0.11; 26.72) (1.56; 0.22; 27.80)	(0.41; 0.53; 19.87) (0.03; 0.86; 23.39)	(1.65; 0.21; 23.60) (4.84; 0.04; 35.73)
Pf (L/R)	(1.15; 0.29; 46.84) (0.74; 0.40; 52.89)	(1.14; 0.30; 46.83) (0.29; 0.59; 52.02)	(2.21; 0.15; 48.92) (1.78; 0.19; 54.72)	(3.60; 0.07; 51.41) (0.28; 0.60; 52.03)	(4.66; 0.04; 53.14) (1.30; 0.26; 53.88)	(0.77; 0.39; 46.06) (0.00; 0.95; 51.49)	(0.10; 0.76; 44.62) (0.23; 0.64; 51.92)
VAmc (L/R)	(0.67; 0.42; 46.21) (1.16; 0.29; 40.47)	(2.49; 0.13; 49.77) (1.06; 0.31; 40.26)	(0.00; 0.97; 44.77) (0.00; 0.96; 37.73)	(3.24; 0.08; 51.11) (0.64; 0.43; 39.28)	(0.91; 0.50; 46.71) (3.38; 0.08; 45.15)	(0.08; 0.77; 44.95) (0.29; 0.59; 38.45)	(0.63; 0.43; 46.12) (2.08; 0.16; 42.50)
MDl (L/R)	(0.50; 0.49; 19.89) (0.31; 0.58; 30.24)	(1.29; 0.27; 22.29) (0.03; 0.85; 29.47)	(1.40; 0.25; 22.62) (1.26; 0.27; 37.76)	(1.43; 0.24; 22.70) (0.01; 0.90; 29.41)	(0.22; 0.64; 18.99) (0.77; 0.39; 31.49)	(0.02; 0.88; 18.36) (0.05; 0.82; 29.52)	(0.38; 0.54; 19.51) (1.83; 0.19; 34.18)
CeM (L/R)	(1.00; 0.33; 39.22) (1.26; 0.27; 28.33)	(2.79; 0.11; 43.12) (0.80; 0.38; 27.03)	(0.69; 0.41; 38.48) (0.06; 0.81; 24.88)	(2.18; 0.15; 41.84) (0.02; 0.90; 24.75)	(2.13; 0.16; 41.74) (1.11; 0.30; 27.90)	(0.15; 0.70; 37.15) (0.13; 0.72; 25.10)	(0.11; 0.74; 37.06) (0.52; 0.48; 26.25)
VA (L/R)	(1.40; 0.25; 59.07) (0.75; 0.39; 65.06)	(0.25; 0.62; 57.20) (0.00; 0.99; 64.01)	(0.00; 0.96; 56.78) (0.14; 0.71; 64.22)	(4.95; 0.03; 63.29) (0.79; 0.38; 65.12)	(0.27; 0.60; 57.25) (3.07; 0.09; 67.95)	(0.01; 0.93; 58.49) (0.55; 0.46; 64.02)	(1.76; 0.20; 59.63) (1.54; 0.23; 66.10)

Table 3 (continued)

	N° Attacks	Attacks duration	Severity of pain	HIT-6	MIDAS	ASC-12	Days since the last attack
MV(Re) (L/R)	(0.14; 0.72; 51.73) (0.06; 0.81; 18.00)	(2.59; 0.12; 56.03) (0.68; 0.42; 19.98)	(0.10; 0.75; 51.67) (0.01; 0.95; 17.83)	(0.39; 0.54; 52.22) (0.42; 0.52; 19.15)	(0.50; 0.49; 52.42) (0.41; 0.53; 19.13)	(1.04; 0.32; 53.41) (0.51; 0.48; 19.46)	(0.28; 0.60; 52.02) (0.06; 0.80; 18.01)
VM (L/R)	(0.02; 0.90; 21.68) (1.19; 0.28; 47.63)	(0.90; 0.35; 24.37) (0.52; 0.48; 46.24)	(0.00; 0.96; 21.63) (3.41; 0.08; 51.70)	(4.06; 0.05; 32.58) (0.62; 0.44; 46.45)	(2.27; 0.14; 28.14) (0.51; 0.48; 46.23)	(0.01; 0.93; 21.65) (0.55; 0.46; 46.31)	(0.01; 0.93; 21.65) (1.04; 0.32; 47.33)
CL (L/R)	(0.36; 0.55; 17.90) (0.20; 0.66; 44.25)	(2.92; 0.10; 25.43) (0.20; 0.66; 44.26)	(1.32; 0.26; 20.91) (0.02; 0.88; 43.86)	(0.42; 0.52; 18.10) (0.94; 0.34; 45.84)	(1.11; 0.30; 20.28) (0.26; 0.61; 44.39)	(1.76; 0.20; 22.20) (0.41; 0.53; 44.71)	(0.27; 0.61; 17.62) (1.01; 0.32; 45.98)
PuL (L/R)	(0.32; 0.58; 52.01) (0.86; 0.36; 61.11)	(2.41; 0.13; 55.68) (1.05; 0.32; 61.39)	(0.12; 0.73; 51.64) (1.72; 0.20; 62.36)	(0.14; 0.71; 51.68) (1.98; 0.17; 63.73)	(2.05; 0.16; 55.08) (3.35; 0.08; 64.53)	(10.23; 0.00; 65.51) (0.06; 0.81; 59.86)	(0.13; 0.72; 51.65) (0.33; 0.57; 60.29)
Pt (L/R)	(0.02; 0.89; 42.87) (2.91; 0.10; 49.67)	(0.54; 0.47; 44.04) (0.05; 0.83; 43.93)	(0.00; 0.95; 42.84) (3.15; 0.09; 50.10)	(0.33; 0.57; 43.57) (0.11; 0.74; 44.06)	(0.27; 0.60; 43.45) (0.41; 0.53; 44.72)	(0.03; 0.86; 42.90) (0.31; 0.58; 44.50)	(0.24; 0.63; 43.37) (1.65; 0.21; 47.29)
AV (L/R)	(1.57; 0.22; 40.13) (0.60; 0.44; 50.55)	(0.53; 0.47; 37.70) (0.06; 0.81; 49.47)	(0.53; 0.47; 37.70) (0.10; 0.75; 49.56)	(0.67; 0.42; 38.04) (0.64; 0.43; 50.63)	(0.02; 0.89; 36.42) (0.21; 0.65; 49.78)	(0.58; 0.45; 37.68) (0.17; 0.68; 49.70)	(3.06; 0.09; 43.31) (5.89; 0.02; 59.02)
Pc (L/R)	(1.10; 0.30; 41.07) (0.22; 0.64; 45.36)	(0.38; 0.54; 39.40) (0.31; 0.58; 45.55)	(0.09; 0.77; 38.69) (0.27; 0.61; 45.47)	(5.47; 0.03; 49.52) (1.48; 0.24; 47.95)	(2.02; 0.17; 43.06) (5.85; 0.02; 55.32)	(0.08; 0.78; 38.66) (0.00; 0.95; 44.89)	(0.11; 0.74; 38.75) (2.65; 0.21; 50.16)
VLp (L/R)	(1.12; 0.30; 43.68) (2.56; 0.12; 56.34)	(0.08; 0.79; 41.33) (0.05; 0.82; 51.97)	(0.08; 0.78; 41.34) (2.10; 0.16; 55.61)	(1.74; 0.20; 44.97) (1.22; 0.28; 54.10)	(0.60; 0.45; 42.53) (3.28; 0.08; 57.46)	(1.64; 0.21; 44.78) (0.13; 0.73; 52.11)	(2.09; 0.16; 45.69) (0.54; 0.47; 52.89)
LP (L/R)	(1.11; 0.30; 37.98) (0.05; 0.82; 43.36)	(1.09; 0.31; 37.94) (3.48; 0.07; 50.18)	(0.09; 0.76; 35.47) (0.47; 0.50; 44.29)	(0.00; 0.99; 35.23) (1.49; 0.23; 46.43)	(0.29; 0.59; 35.97) (0.27; 0.61; 43.85)	(0.15; 0.70; 35.61) (0.34; 0.56; 43.99)	(0.47; 0.50; 36.43) (0.15; 0.70; 43.59)
LD (L/R)	(0.15; 0.70; 20.15) (0.30; 0.51; 25.95)	(1.85; 0.18; 25.20) (0.82; 0.37; 27.44)	(1.20; 0.28; 23.34) (4.62; 0.04; 36.76)	(0.22; 0.64; 20.37) (1.91; 0.28; 30.37)	(0.02; 0.90; 19.73) (1.02; 0.32; 28.01)	(2.11; 0.16; 25.94) (0.26; 0.62; 25.82)	(0.52; 0.48; 21.32) (0.11; 0.74; 25.39)
Whole thalamus (L/R)	(1.17; 0.29; 51.96) (1.23; 0.28; 55.14)	(0.97; 0.33; 51.60) (0.03; 0.87; 52.97)	(0.07; 0.80; 49.85) (2.40; 0.13; 57.05)	(2.40; 0.13; 54.13) (0.39; 0.54; 53.64)	(1.18; 0.29; 51.99) (2.66; 0.12; 57.44)	(0.14; 0.71; 49.99) (0.03; 0.86; 52.98)	(1.36; 0.25; 52.30) (2.55; 0.12; 57.28)

that microstructural/physiological perturbations can exist without detectable macrostructural volume loss. Current and prior neuroimaging and electrophysiological findings suggest that one of the pathogenic mechanisms of migraine is influenced by intricate disruption of thalamocortical connectivity and the temporal activation of neural networks. This impaired brain pattern, termed thalamocortical dysrhythmia, encompasses morphological and functional changes in the thalamus that result in insufficient cortical functional regulation, as demonstrated by electrophysiological studies [1, 4, 5, 52]. This dysrhythmia may result in disturbances in the processing of both painful and non-painful information, potentially leading to neurological symptoms [2].

This study has some limitations. First, we did not evaluate the same individuals at various stages of the migraine cycle, encompassing pre-ictal, ictal, and post-ictal phases. Second, the study design lacked long-term monitoring to assess whether spontaneous fluctuations or prophylactic treatments may cause macrostructural plasticity in the thalamus. Finally, despite our sample size being larger than that of other comparable research and the use of a more stringent statistical approach, the relatively small number of participants may restrict the generalizability of our results. Although no formal power analysis was

Table 4 FDR-corrected p values for uncorrected significant associations (p-uncorrected < 0.05) from Table 3

	***N°* Attacks**	**Attacks duration**	**Severity of pain**	**HIT-6**	**MIDAS**	**ASC-12**	**Days since the last attack**
LGN (L/R)	0.72; 0.72	n.s. (= *not significant*)	0.47; 0.41	0.92; 0.71	0.66; 0.58	0.97; 0.97	0.68; 0.68
MGN (L/R)	0.72; 0.72	n.s.	0.41; 0.41	0.94; 0.71	0.90; 0.87	0.97; 0.97	0.84; 0.84
PuI (L/R)	0.93; 0.93	n.s.	0.75; 0.68	0.91; 0.67	0.58; 0.58	0.97; 0.97	0.84; 0.68
PuM (L/R)	0.83; 0.93	n.s.	0.68; 0.74	0.94; 0.67	0.64; 0.66	0.97; 0.97	0.80; 0.68
L-Sg (L/R)	0.72; 0.72	n.s.	0.98; 0.98	0.67; 0.94	0.69; 0.82	0.97; 0.97	0.70; 0.80
VPL (L/R)	0.81; 0.72	n.s.	0.98; 0.47	0.67; 0.71	0.74; 0.66	0.97; 0.97	0.80; 0.68
CM (L/R)	0.83; 0.93	n.s.	0.93; 0.41	0.67; 0.67	0.58; 0.66	1.00; 0.97	0.97; 0.98
VLa (L/R)	0.72; 0.72	n.s.	0.98; 0.61	0.67; 0.67	0.78; 0.58	0.97; 0.97	0.68; 0.80
PuA (L/R)	0.90; 0.93	n.s.	0.47; 0.78	0.74; 0.94	0.78; 0.74	0.97; 0.97	0.70; 0.70
MDm (L/R)	0.83; 0.93	n.s.	0.76; 0.75	0.67; 0.94	0.58; 0.66	0.97; 0.97	0.68; 0.68
Pf (L/R)	0.72; 0.81	n.s.	0.61; 0.67	0.67; 0.81	0.71; 0.66	0.97; 0.97	0.84; 0.84
VAmc (L/R)	0.81; 0.72	n.s.	0.98; 0.98	0.67; 0.71	0.67; 0.58	0.97; 0.97	0.80; 0.68
MDl (L/R)	0.83; 0.83	n.s.	0.68; 0.68	0.67; 0.94	0.76; 0.69	0.97; 0.97	0.84; 0.68
CeM (L/R)	0.74; 0.72	n.s.	0.78; 0.98	0.67; 0.94	0.58; 0.66	0.97; 0.97	0.84; 0.80
VA (L/R)	0.72; 0.72	n.s.	0.98; 0.98	0.67; 0.71	0.75; 0.58	0.97; 0.97	0.68; 0.68
MV(Re) (L/R)	0.81; 0.93	n.s.	0.98; 0.98	0.77; 0.77	0.74; 0.74	0.97; 0.97	0.84; 0.86
VM (L/R)	0.93; 0.72	n.s.	0.98; 0.47	0.67; 0.71	0.58; 0.74	0.97; 0.97	0.97; 0.74
CL (L/R)	0.83; 0.89	n.s.	0.68; 0.98	0.77; 0.71	0.66; 0.75	0.97; 0.97	0.84; 0.74
PuL (L/R)	0.83; 0.79	n.s.	0.98; 0.67	0.91; 0.67	0.58; 0.58	0.20; 0.97	0.84; 0.84
Pt (L/R)	0.93; 0.72	n.s.	0.98; 0.47	0.79; 0.91	0.72; 0.74	0.97; 0.97	0.84; 0.68
AV (L/R)	0.72; 0.82	n.s.	0.85; 0.98	0.71; 0.71	0.90; 0.76	0.97; 0.97	0.68; 0.68
Pc (L/R)	0.72; 0.89	n.s.	0.98; 0.98	0.67; 0.67	0.58; 0.58	0.97; 0.97	0.84; 0.68
VLp (L/R)	0.72; 0.72	n.s.	0.98; 0.61	0.67; 0.67	0.74; 0.58	0.97; 0.97	0.68; 0.80
LP (L/R)	0.72; 0.93	n.s.	0.98; 0.86	0.94; 0.67	0.75; 0.75	0.97; 0.97	0.80; 0.84
LD (L/R)	0.90; 0.83	n.s.	0.68; 0.41	0.85; 0.67	0.90; 0.66	0.97; 0.97	0.80; 0.84

conducted, our sample size is consistent with previous morphometric studies using FreeSurfer thalamic segmentation in migraine. However, we cannot exclude that subtle volumetric differences exist below our detection threshold. Given the use of covariates (age, sex, TIV) and the probabilistic, modulated estimation of volumes via FreeSurfer, statistical sensitivity may have been further reduced.

Moreover, although healthy controls were recruited from among medical students and healthcare professionals to allow strict application of health screening criteria,

Table 5 Ophthalmological features for healthy controls (HCs) and patients with migraine without aura scanned during migraine-free intervals (MO)

	HCs (*n* = 30)	MO (*n* = 30)
Visual Acuity (Decimal Snellen Equivalent)	1.00 ± 0.00	1.00 ± 0.00
Intraocular pressure (mmHg)	13.40 ± 1.30	12.80 ± 1.70
Refractive error (dioptre spherical equivalent)	0.75 ± 0.25	0.25 ± 0.25
Chromatic perception (Ishihara plates ratio)	1.00 ± 0.00	1.00 ± 0.00

Data are presented as mean ± standard deviation

this may further limit the extension of our findings to the general population.

Conclusions

In conclusion, our investigation found no macrostructural volumetric anomalies in the thalami and their subnuclei bilaterally in patients with MO during the pain-free phase and without receiving preventative medication, in comparison to healthy controls. Similar patterns—absence of macrostructural alterations alongside functional and microstructural abnormalities—have been reported in other primary headache disorders such as cluster headache, as well as in neurological conditions like schizophrenia and restless legs syndrome [53–55]. More studies should be devoted to the investigation of structural changes in patients with migraine with aura and its clinical subtypes, and in those who have severe migraine symptoms that necessitate the use of preventive medications. Moreover, future research combining multimodal imaging techniques with longitudinal study designs will be essential to further elucidate the dynamic neurobiological underpinnings of migraine and guide the development of personalized therapeutic strategies.

Abbreviations

BOLD Blood oxygen level dependent
FC Functional connectivity
FDR False discovery rate
GLM General linear model
MRI Magnetic resonance imaging
HCs Healthy controls
MO Migraine without aura

Supplementary Information

The online version contains supplementary material available at https://doi.org/10.1186/s10194-025-02196-9.

Supplementary Material 1

Acknowledgements

The contribution of the G.B. Bietti Foundation to this paper was supported by the Italian Ministry of Health and Fondazione Roma.

Author contributions

IG, ADR, and GC made substantial contributions to protocol development, interpretation of data as well as in drafting the manuscript. MA, DC, FCar, VP, LZ and VDP were implied in the interpretation of data as well as in drafting the

Table 6 Cohen's d effect sizes for each thalamic subregion

	Effect size
LGN (L/R)	0.71; 0.63
MGN (L/R)	0.46; 0.36
PuI (L/R)	0.47; 0.53
PuM (L/R)	0.45; 0.58
L-Sg (L/R)	0.34; 0.06
VPL (L/R)	0.41; 0.12
CM (L/R)	0.49; 0.33
VLa (L/R)	0.70; 0.53
PuA (L/R)	0.47; 0.42
MDm (L/R)	0.25; 0.48
Pf (L/R)	0.41; 0.09
VAmc (L/R)	0.58; 0.59
MDl (L/R)	0.51; 0.35
CeM (L/R)	0.42; 0.36
VA (L/R)	0.64; 0.54
MV(Re) (L/R)	0.27; 0.37
VM (L/R)	0.21; 0.00
CL (L/R)	0.26; 0.47
PuL (L/R)	0.44; 0.30
Pt (L/R)	0.55; 0.32
AV (L/R)	0.35; 0.34
Pc (L/R)	0.51; 0.54
VLp (L/R)	0.68; 0.45
LP (L/R)	0.73; 0.42
LD (L/R)	0.18; 0.29
Whole_thalamus (L/R)	0.61; 0.47

manuscript; AP, GG, GS, CA, and FCas contributed to participant enrolment and recording. ADR and FCar were implied in data processing, analysis, and statistics.

Funding
The authors did not receive funding for the design of the study and collection, analysis, and interpretation of data and in writing the manuscript.

Data availability
The informed consent signed by all participants in this study did not include a provision stating that individual raw data can be made publicly accessible. Therefore, in agreement with the Italian data protection law, individual de-identified participant raw data cannot be shared publicly. Researchers meeting the criteria for access to confidential data may access the data upon request, involving the documentation of data access.

Declarations

Ethics approval and consent to participate
All the participants provided written informed consent to participate in the study, which was approved by the ethical review board of the Faculty of Medicine at the University of Rome, Italy (N° 0295/2023).

Consent for publication
Not applicable.

Competing interests
The authors declare no competing interests.

Author details
[1]Department of Radiological Sciences, Oncology and Pathology, Sapienza University of Rome, Viale dell'Università 30, 00185 Rome, Italy
[2]IRCCS – Fondazione Bietti, Clinical and Research Center of Neurophthalmology and Genetic and Rare Diseases of the Eye, Rome, Italy
[3]Department of Human Neurosciences, Sapienza University of Rome, Rome, Italy
[4]Department of Medico-Surgical Sciences and Biotechnologies, Sapienza University of Rome Polo Pontino ICOT, Latina, Italy
[5]Department of Medicine and Health Sciences "Vincenzo Tiberio", University of Molise, Campobasso, Italy
[6]Neuroradiology Unit, Policlinico Umberto I, Rome, Italy
[7]Departmental Faculty of Medicine, UniCamillus-Saint Camillus International University of Health Sciences, Rome, Italy

Received: 28 July 2025 / Accepted: 14 October 2025
Published online: 07 November 2025

References

1. Porcaro C, Di Lorenzo G, Seri S et al (2017) Impaired brainstem and thalamic high-frequency oscillatory EEG activity in migraine between attacks. Cephalalgia 37:915–926. https://doi.org/10.1177/0333102416657146
2. Russo A, Coppola G, Pierelli F et al (2018) Pain perception and migraine. Front Neurol 9:576. https://doi.org/10.3389/fneur.2018.00576
3. Puledda F, Viganò A, Sebastianelli G et al (2023) Electrophysiological findings in migraine may reflect abnormal synaptic plasticity mechanisms: a narrative review. Cephalalgia 43. https://doi.org/10.1177/03331024231195780
4. Coppola G, Iacovelli E, Bracaglia M et al (2013) Electrophysiological correlates of episodic migraine chronification: evidence for thalamic involvement. J Headache Pain 14:76
5. Coppola G, Ambrosini A, Di Clemente L et al (2007) Interictal abnormalities of gamma band activity in visual evoked responses in migraine: an indication of thalamocortical dysrhythmia? Cephalalgia 27:1360–1367. https://doi.org/10.1111/j.1468-2982.2007.01466.x
6. Coppola G, Bracaglia M, Di Lenola D et al (2016) Lateral Inhibition in the somatosensory cortex during and between migraine without aura attacks: correlations with thalamocortical activity and clinical features. Cephalalgia: Int J Headache 36:568–578. https://doi.org/10.1177/0333102415610873
7. Restuccia D, Vollono C, Del Piero I et al (2012) Somatosensory high frequency oscillations reflect clinical fluctuations in migraine. Clin Neurophysiol 123:2050–2056. https://doi.org/10.1016/j.clinph.2012.03.009
8. Shields KG, Goadsby PJ (2006) Serotonin receptors modulate trigeminovascular responses in ventroposteromedial nucleus of thalamus: a migraine target? Neurobiol Dis 23:491–501
9. Summ O, Charbit AR, Andreou AP, Goadsby PJ (2010) Modulation of nocioceptive transmission with calcitonin gene-related peptide receptor antagonists in the thalamus. Brain 133:2540–2548
10. Shields KG, Goadsby PJ (2005) Propranolol modulates trigeminovascular responses in thalamic ventroposteromedial nucleus: a role in migraine? Brain 128:86–97. https://doi.org/10.1093/brain/awh298
11. Andreou AP, Shields KG, Goadsby PJ (2010) GABA and valproate modulate trigeminovascular nociceptive transmission in the thalamus. Neurobiol Dis 37:314–323
12. Andreou AP, Goadsby PJ (2011) Topiramate in the treatment of migraine: a Kainate (glutamate) receptor antagonist within the trigeminothalamic pathway. Cephalalgia: Int J Headache 31:1343–1358
13. Noseda R, Kainz V, Jakubowski M et al (2010) A neural mechanism for exacerbation of headache by light. Nat Neurosci 13:239–245
14. Stankewitz A, Schulz E, May A (2013) Neuronal correlates of impaired habituation in response to repeated trigemino-nociceptive but not to olfactory input in migraineurs: an fMRI study. Cephalalgia: Int J Headache 33:256–265
15. Russo A, Marcelli V, Esposito F et al (2014) Abnormal thalamic function in patients with vestibular migraine. Neurology 82:2120–2126
16. Coppola G, Tinelli E, Lepre C et al (2014) Dynamic changes in thalamic microstructure of migraine without aura patients: a diffusion tensor magnetic resonance imaging study. Eur J Neurology: Official J Eur Federation Neurol Soc 21:287–e13. https://doi.org/10.1111/ene.12296
17. Marciszewski KK, Meylakh N, Pietro FD et al (2019) Fluctuating regional brainstem diffusion imaging measures of microstructure across the migraine cycle. https://doi.org/10.1523/ENEURO.0005-19.2019. eneuro ENEURO.0005-19.2019
18. Coppola G, Di Renzo A, Tinelli E et al (2016) Thalamo-cortical network activity between migraine attacks: insights from MRI-based microstructural and functional resting-state network correlation analysis. J Headache Pain 17:100. https://doi.org/10.1186/s10194-016-0693-y
19. Magon S, May A, Stankewitz A et al (2015) Morphological abnormalities of thalamic subnuclei in migraine: A multicenter MRI study at 3 Tesla. J Neuroscience: Official J Soc Neurosci 35:13800–13806
20. Hebestreit JM, May A (2017) Topiramate modulates trigeminal pain processing in thalamo-cortical networks in humans after single dose administration. PLoS ONE 12:e0184406. https://doi.org/10.1371/journal.pone.0184406
21. Hebestreit JM, May A (2017) The enigma of site of action of migraine preventives: no effect of Metoprolol on trigeminal pain processing in patients and healthy controls. J Headache Pain 18:116. https://doi.org/10.1186/s10194-017-0827-x
22. Filippi M, Messina R, Bartezaghi M et al (2023) The effect of erenumab on brain network function in episodic migraine patients: a randomized, placebo-controlled clinical trial (RESET BRAIN). J Neurol 270:5600–5612. https://doi.org/10.1007/s00415-023-11879-9
23. Schwedt TJ, Nikolova S, Dumkrieger G et al (2022) Longitudinal changes in functional connectivity and pain-induced brain activations in patients with migraine: a functional MRI study pre- and post- treatment with erenumab. J Headache Pain 23:159. https://doi.org/10.1186/s10194-022-01526-5
24. Nikolova S, Chong CD, Dumkrieger GM et al (2023) Longitudinal differences in iron deposition in periaqueductal Gray matter and anterior cingulate cortex are associated with response to erenumab in migraine. Cephalalgia 43:3331024221144783. https://doi.org/10.1177/03331024221144783
25. Messina R, Rocca MA, Valsasina P et al (2022) Clinical correlates of hypothalamic functional changes in migraine patients. Cephalalgia 42:279–290. https://doi.org/10.1177/03331024211046618
26. Messina R, Rocca MA, Colombo B et al (2018) Gray matter volume modifications in migraine. Neurology 91:e280–e292. https://doi.org/10.1212/WNL.0000000000005819
27. Naguib LE, Abdel Azim GS, Abdellatif MA (2021) A volumetric magnetic resonance imaging study in migraine. Egypt J Neurol Psychiatry Neurosurg 57:116. https://doi.org/10.1186/s41983-021-00372-7
28. Shin KJ, Lee HJ, Park KM (2019) Alterations of individual thalamic nuclei volumes in patients with migraine. J Headache Pain 20:112. https://doi.org/10.1186/s10194-019-1063-3

29. Maniyar F, Sprenger T, Monteith T et al (2014) Brain activations in the premonitory phase of nitroglycerin-triggered migraine attacks. Brain 137:232–241
30. Denuelle M, Fabre N, Payoux P et al (2007) Hypothalamic activation in spontaneous migraine attacks. Headache 47:1418–1426
31. Schulte LH, May A (2016) The migraine generator revisited: continuous scanning of the migraine cycle over 30 days and three spontaneous attacks. Brain 139:1987–1993. https://doi.org/10.1093/brain/aww097
32. Sebastianelli G, Atalar AÇ, Cetta I et al (2024) Insights from triggers and prodromal symptoms on how migraine attacks start: the threshold hypothesis. Cephalalgia 44:3331024241287224. https://doi.org/10.1177/03331024241287224
33. Iglesias JE, Insausti R, Lerma-Usabiaga G et al (2018) A probabilistic atlas of the human thalamic nuclei combining ex vivo MRI and histology. NeuroImage 183:314–326. https://doi.org/10.1016/j.neuroimage.2018.08.012
34. Wang J, Li T, Sabel BA et al (2016) Structural brain alterations in primary open angle glaucoma: a 3T MRI study. Sci Rep 6:18969. https://doi.org/10.1038/srep18969
35. Headache Classification Committee of the International Headache Society (IHS) (2018) The International Classification of Headache Disorders, 3rd ed. Cephalalgia 38:1–211. https://doi.org/10.1177/0333102417738202
36. Chong CD, Aguilar M, Schwedt TJ (2020) Altered hypothalamic region covariance in migraine and cluster headache: A structural MRI study. Headache 60:553–563. https://doi.org/10.1111/head.13742
37. Reuter M, Rosas HD, Fischl B (2010) Highly accurate inverse consistent registration: a robust approach. NeuroImage 53:1181–1196. https://doi.org/10.1016/j.neuroimage.2010.07.020
38. Ségonne F, Dale AM, Busa E et al (2004) A hybrid approach to the skull stripping problem in MRI. NeuroImage 22:1060–1075. https://doi.org/10.1016/j.neuroimage.2004.03.032
39. Han X, Jovicich J, Salat D et al (2006) Reliability of MRI-derived measurements of human cerebral cortical thickness: the effects of field strength, scanner upgrade and manufacturer. NeuroImage 32:180–194. https://doi.org/10.1016/j.neuroimage.2006.02.051
40. Fischl B, Salat DH, van der Kouwe AJW et al (2004) Sequence-independent segmentation of magnetic resonance images. Neuroimage 23 Suppl 1S69–84. https://doi.org/10.1016/j.neuroimage.2004.07.016
41. Fischl B, Sereno MI, Dale AM (1999) Cortical surface-based analysis. II: Inflation, flattening, and a surface-based coordinate system. NeuroImage 9:195–207. https://doi.org/10.1006/nimg.1998.0396
42. Fischl B, Sereno MI, Tootell RB, Dale AM (1999) High-resolution intersubject averaging and a coordinate system for the cortical surface. Hum Brain Mapp 8:272–284. https://doi.org/10.1002/(sici)1097-0193(1999)8:4%3C272::aid-hbm10%3E3.0.co;2-4
43. Fischl B, Liu A, Dale AM (2001) Automated manifold surgery: constructing geometrically accurate and topologically correct models of the human cerebral cortex. IEEE Trans Med Imaging 20:70–80. https://doi.org/10.1109/42.906426
44. Fischl B, Dale AM (2000) Measuring the thickness of the human cerebral cortex from magnetic resonance images. Proc Natl Acad Sci U S A 97:11050–11055. https://doi.org/10.1073/pnas.200033797
45. Matharu MS, Good CD, May A et al (2003) No change in the structure of the brain in migraine: a voxel-based morphometric study. Eur J Neurology: Official J Eur Federation Neurol Soc 10:53–57
46. Coppola G, Di Renzo A, Tinelli E et al (2016) Thalamo-cortical network activity during spontaneous migraine attacks. Neurology 87:2154–2160. https://doi.org/10.1212/WNL.0000000000003327
47. Amin FM, Hougaard A, Magon S et al (2018) Altered thalamic connectivity during spontaneous attacks of migraine without aura: A resting-state fMRI study. Cephalalgia 38:1237–1244. https://doi.org/10.1177/0333102417729113
48. Yang Y, Xu H, Deng Z et al (2022) Functional connectivity and structural changes of thalamic subregions in episodic migraine. J Headache Pain 23:119. https://doi.org/10.1186/s10194-022-01491-z
49. Tu Y, Fu Z, Zeng F et al (2019) Abnormal thalamocortical network dynamics in migraine. Neurology 92:e2706–e2716. https://doi.org/10.1212/WNL.0000000000007607
50. Hodkinson DJ, Wilcox SL, Veggeberg R et al (2016) Increased amplitude of thalamocortical Low-Frequency oscillations in patients with migraine. J Neuroscience: Official J Soc Neurosci 36:8026–8036. https://doi.org/10.1523/JNEUROSCI.1038-16.2016
51. Cao ZM, Chen YC, Liu GY et al (2022) Abnormalities of thalamic functional connectivity in patients with migraine: A Resting-State fMRI study. Pain Therapy 11:561–574. https://doi.org/10.1007/S40122-022-00365-1
52. Bjørk MH, Stovner LJ, Engstrøm M et al (2009) Interictal quantitative EEG in migraine: a blinded controlled study. J Headache Pain 10:331–339. https://doi.org/10.1007/s10194-009-0140-4
53. Kraguljac NV, Anthony T, Skidmore FM et al (2019) Micro- and macrostructural white matter integrity in Never-treated and currently unmedicated patients with schizophrenia and effects of short term antipsychotic treatment. Biol Psychiatry Cogn Neurosci Neuroimaging 4:462–471. https://doi.org/10.1016/j.bpsc.2019.01.002
54. Belke M, Heverhagen JT, Keil B et al (2015) DTI and VBM reveal white matter changes without associated Gray matter changes in patients with idiopathic restless legs syndrome. Brain Behav 5:e00327. https://doi.org/10.1002/brb3.327
55. Abagnale C, Di Renzo A, Giuliani G et al (2025) MRI-based analysis of the microstructure of the thalamus and hypothalamus and functional connectivity between cortical networks in episodic cluster headache. J Headache Pain 26:12. https://doi.org/10.1186/s10194-024-01920-1

Publisher's note